Current Research in Food Science 6 (2023) 100451

Contents lists available at ScienceDirect

Current Research in Food Science

journal homepage: www.sciencedirect.com/journal/current-research-in-food-science

HPTLC-based fingerprinting: An alternative approach for fructooligosaccharides metabolism profiling

Luis Francisco Salomé-Abarca [a], Ruth Esperanza Márquez-López [b], Patricia Araceli Santiago-García [b], Mercedes G. López [a,*]

[a] Departamento de Biotecnología y Bioquímica, Centro de Investigación y de Estudios Avanzados del IPN-Unidad Irapuato, Guanajuato, 36824, Mexico
[b] Instituto Politécnico Nacional, Centro Interdisciplinario de Investigación Para el Desarrollo Integral Regional-Unidad Oaxaca, Oaxaca, 71230, Mexico

ARTICLE INFO

Handling Editor: Dr. Quancai Sun

Keywords:
HPTLC
Fructooligosaccharides
Agave
Data extraction
Isomers

ABSTRACT

Fructans are categorized as fructose-based metabolites with no more than one glucose in their structure. *Agave* species possess a mixture of linear and ramified fructans with different degrees of polymerization. Among them, fructooligosaccharides are fructans with low degree of polymerization which might be approachable by high performance thin layer chromatography (HPTLC). Thus, this study used two emblematic *Agave* species collected at different ages as models to explore the feasibility of HPTLC-based fingerprinting to characterize fructooligosaccharides (FOS) production, accumulation, and behavior through time. To do so, high performance anion exchange was also used as analytical reference to determine the goodness and robustness of HPTLC data. The multivariate data analysis showed separation of samples dictated by species and age effects detected by both techniques. Moreover, linear correlations between the increase of the age in agave and their carbohydrate fraction was established in both species by both techniques. Oligosaccharides found to be correlated to species and age factors, these suggest changes in specific carbohydrate metabolism enzymes. Thus, HPTLC was proven as a complementary or stand-alone fingerprinting platform for fructooligosaccharides characterization in biological mixtures. However, the type of derivatizing reagent and the extraction color channel determined the goodness of the model used to scrutinize agavin fructooligosaccharides (aFOS).

1. Introduction

Fructans are categorized as fructose-based metabolites with no more than one glucose in their structure. These compounds are found in all biological kingdoms except in animalia (Versluys et al., 2018). A subclass of fructans, fructooligosaccharides (FOS), are linear oligomers of β (2–1)-linked D-fructose with a maximum degree of polymerization (DP) of 11 (Jaime et al., 2001; Gibson and Roberfroid, 2008). Due to their molecular weight, they can be considered in the class of small molecules (Qiu et al., 2012; Gaudêncio and Pereira, 2015). Linear FOS have two series: α-D-glucopyranosyl-[β-D-fructofuranosyl]n-1-β-fructofuranoside (GFn) and β-D-fructofuranosyl-[β-D-fructofuranosyl]m-1-β-D-fructopy ranose (FmFp); the fructosyl-glucose linkage is always β (2↔1) and fructosyl-fructose linkages are also β (2 → 1) (Gibson and Roberfroid, 2008; Yildiz, 2010). Such fructans are considered multifunctional compounds, which confers them several practical applications in the industry as prebiotics, sweeteners, fat replacers, among others (Santiago-García et al., 2021; Martínez-Gamiño et al., 2022; García--Villalba et al., 2022). Thus, FOS represent the best commercialized group of oligosaccharides in the European market (Nobre et al., 2013; Domínguez et al., 2014).

Additionally, there is a peculiar subclass of FOS, the so called agavin fructooligosaccharides (aFOS), which are present only in *Agave* species. aFOS are characterized by possessing several ramifications in their chemical structure, a mixture of graminans and *neo*-fructans (Mancilla-Margalli and López, 2006; Huazano-García and López, 2018; Aldrete-Herrera et al., 2019). This feature provides aFOS with the largest isomerism rate among FOS (Arrizon et al., 2014; Mellado-Mojica and López, 2012). In addition, *Agave* species possess a mixture of different types of linear and branched fructans (Mellado-Mojica and López, 2012), which makes them an excellent model to perform fingerprinting analyses for characterizing their behavior.

In this context, the chemical analysis of fructan comprise several chromatographic techniques such as ultra-high-performance liquid

* Corresponding author.
E-mail address: mercedes.lopez@cinvestav.mx (M.G. López).

https://doi.org/10.1016/j.crfs.2023.100451
Received 28 November 2022; Received in revised form 9 January 2023; Accepted 30 January 2023
Available online 31 January 2023

chromatography (UHPLC), hydrophilic interaction chromatography (HILIC), high-performance anion-exchange chromatography (HPAEC), gas chromatography (GC), size exclusion chromatography (SEC), capillary electrophoresis (CE), and thin layer chromatography (TLC). All these techniques have been coupled to several types of detectors. For instance, UHPLC and HILIC have been coupled with evaporative light scattering detectors (Matros et al., 2019). On the other hand, HPAEC is hyphenated to a pulsed amperometric detector, which is the most widely used technique for fructan detection and quantitation (Shiomi et al., 1991; Huazano-García and López, 2018). Gas chromatography has been coupled to mass spectrometry and it is mainly used to get structural information from partially methylated alditol acetate derivatives (Mancilla-Margalli and López, 2006; Ruíz-Matute et al., 2011). Other spectrometric techniques such as near infrared (NIR) or Fourier transformed-middle infrared spectroscopy (FT-MIR) have also been employed for the analysis and characterization of fructans (Shetty et al., 2012; Cozzolino et al., 2014). Most of these techniques have been approached by chemometrics means in biological or quality control studies.

However, historically, the development of sugar analysis by paper chromatography allowed for the first proper separation of sugars (Kowkabany, 1954; Matros et al., 2019). Subsequently, the evolution of TLC to high-performance thin layer chromatography (HPTLC) has provided advanced separation and faster analytical speed compared to other liquid chromatography techniques. Nonetheless, the current state of TLC and HPTLC analysis of FOS still lacking a general approach that allows a direct comparison between different fructan studies (Benkeblia, 2013; Matros et al., 2019).

TLC analysis of fructans has been mainly approached by visual inspection, which interpretation vary from analyst to analyst depending on their experience. TLC and HPTLC analyses have also been used for densitometric analysis to quantitate fructans (Cheong et al., 2014). These applications have allowed for the visual distinction of fructans' plant origin, qualitatively and quantitatively (Alvarado et al., 2014). Some examples include the profiling of apple juice supplemented with agave fructans, inulin, and oligofructose (González-Herrera et al., 2016), root-tubers of *Asphodelus ramosus* (Madia et al., 2021), fructans in *Aloe barbadensis* (Salinas et al., 2016), among others. However, sample application and chromatographic development conditions vary a lot among studies making difficult to compare data between them (Mellado-Mojica and López, 2012; Alvarado et al., 2014; Pérez-López et al., 2021). In addition, HPTLC data has never been explored for the targeted fingerprinting characterization of FOS.

In this context, nowadays HPTLC has been coupled with multivariate data analysis through data extraction and multivariate data analysis software (Fichou et al., 2016). All the colorful bands detected on the chromatographic plates represents thousands of pixels used as variables (Komsta, 2012). Furthermore, the availability of several derivatizing reagents results in contrasting coloration patterns representing different data sets providing complementing information (Ristivojević et al., 2014). This potential has been demonstrated for numerous plant materials with many types of diverse metabolites such as volatile compounds, saponins, anthraquinones, and glycosilflavones (Ge et al., 2018; Salomé-Abarca et al., 2018; Oomen et al., 2020). Thus, the aim of this research was to test the feasibility of HPTLC-based fingerprinting for aFOS metabolism characterization. To carry out such an analysis two emblematic and recently explored *Agave* species collected at six ages were chosen as biological models. Finally, HPTLC data was compared with that of HPAEC-PAD, considered as analytical reference, in terms of group separation, predictive power, and statistical significance of obtained models from both techniques.

2. Experimental

2.1. Plant material

Samples consisted of specimens of *Agave angustifolia* Haw. (Agavaceae) and *Agave potatorum* Zucc. (Agavaceae) collected at San Esteban Amatlán, Oaxaca, Mexico (N 16°23′, W 96°30′) and Infiernillo, Zaachila Oaxaca, Mexico (N 16°89′, W 97°19′), respectively. Specimens of both species were collected at ages ranging from one to six years old. Three samples were collected per age making a total of 36 samples per both species. The age of *A. angustifolia* specimens was counted from the plant shoot ("el hijuelo") plantation at the field. The age of *A. potatorum* specimens was counted from the moment of the seed ("la semilla") plantation at the field. After sampling (no longer than 6 h), all the samples were cut into sections as previously described (Arrizon et al., 2010). Then, the samples were stored in plastic bags at −20 °C for later analysis.

2.2. Sample preparation

Total fructans were extracted as previously reported with some modifications. Briefly, 100 g of agave fibers, taken from the center of the agave pine, was extracted with 100 mL aqueous ethanol [80%] under continuous stirring for 1 h at 60 °C. Afterwards, the extract was filtered, and the remaining plant material was sequentially re-extracted two times with 100 mL of distilled water for 30 min at 60 °C. At the end of the extractions all the supernatants were mixed. Chloroform was used to eliminate non-polar components from the extract. The aqueous phase was concentrated by evaporation with a rotary evaporator R-200 (Büchi, Westbury, New York) and spray dried. To do so, a spray dryer device ADL 3115 (Yamato, Tokyo, Japan) was employed. Samples were placed into the drying chamber by means of a peristaltic pump at a flow rate of 3 mL/min. The temperature of the drying inlet was set to 140 °C. The temperature of the outlet exhaust air was 80 °C with atomization pressure of 0.25 MPa. Samples were stored in a desiccator for further analysis.

FOS fractions were obtained from dried fructans by alcohol precipitation. For this, 500 mg of fructan were dissolved in five mL of distilled water. Subsequently, 25 mL of absolute ethanol were added to the fructan solution, and the mixture was vigorously shaken for 2 min. The solution was stored at 4 °C for 24 h to obtain a precipitated suspension. The oligosaccharides contained in the supernatant were separated from higher DP compounds by centrifugation at 3000×*g* for 6 min. The supernatant containing the FOS fraction was recovered and taken to total dryness by vacuum evaporation. Finally, five mL of distilled water were added to the sample to be lyophilized with a freeze dryer (FreeZone 4.5, Labconco, Kansas, Missouri) and a white powder was obtained.

2.3. High performance anion exchange chromatography coupled to pulsed amperometric detection (HPAEC-PAD)

The fructan profiles of all specimens were performed in a liquid ion-exchange chromatograph DIONEX ICS-3000 (Thermoscientific, Waltham, MA, USA). The system was equipped with a Carbopac PA-200 (40 × 250 mm) column and a precolumn (40 × 25 mm). The gradient for sample separation used NaOH [0.23 M], CH_3COONa [0.5 M], and water at constant flow of 2 mL/min. The separation started with a gradient 70% of water (A), 30% of aqueous NaOH (B), and 0% of NaOH/CH3COONa (C), the following percentual ratios of A and B were 50:50 (5 min), 45:40 (8 min), 40:30 (27 min), 30:20 (15 min), 15:10 (10 min), and 50:50 (10 min), respectively; when the sum of A and B was not 100%, the rest of the mobile was composed of C. The metabolites were

detected with an amperometric detector; the potential used for amperometric detection was +0.1, −2.0, +0.6 y −0.1 V for E1 (400 ms), E2 (20 ms), E3 (20 ms), and E4 (60 ms), respectively (Mellado-Mojica and López, 2012). All obtained results were expressed in nC vs time. Additionally, standards of glucose, fructose, sucrose, 1-kestose, 1-nystose, and 1-F fructofuranosylnystose (DP5) [12.5 μg/mL] were injected to properly determine the degree of polymerization in the analyzed fructans. Another control sample to determine apparent degree of polymerization was a commercial raftiline (RNE)-GR sample subjected to ethanol precipitation, obtained from Orafti. All samples, including standard compounds, were filtered through a 0.22 μm (Millipore®, Burlington, MA, USA) nylon membrane.

2.4. High-performance thin layer chromatography (HPTLC)

For HPTLC analysis, the FOS fractions were firstly dissolved in 300 μL of distilled water and then taken up to 1 mL with 700 μL of absolute ethanol (room temperature) in a 2 mL glass vial. The samples were softly mixed and then ultra-sonicated for 2 min.

Silica gel HPTLC plates (20 × 10 cm, F_{254}) were purchased from Merck (Darmstadt, Germany). Samples were processed using a CAMAG-HPTLC system (Muttenz, Switzerland) equipped with an automatic ATS4-TLC sampler, an ADC2-TLC developer, an automatic derivatizer (version 1.0 AT), and a TLC visualizer (version 2). Due to sample density, a concentration of 7 mg/mL was the optimum sample concentration to be properly taken by the ATS4 syringe. The optimized conditions for sample suction and application conditions were filling speed: 8 μL/s, predosage volume: 200 nL, retraction volume: 20 nL, dosage speed: 70 nL/s, rinsing cycles/vacuum: 1/8 s, filling cycles/vacuum: 1/1 s. The washing solution for the syringe and needle consisted of only distilled water.

Different volumes of the aFOS extracts were applied on the plate and the best patterns were produced from 5 μL. Thus, this volume of each sample was spotted as 6 mm bands. For the chromatographic analysis, seventeen samples were spotted on each plate leaving 8 mm distance from the bottom of the plate and 20 mm from the left and right edges of the plate. The distance between bands was 10 mm. The distances were set to be calculated from the center of the band. Thus, thirteen agave samples were applied per HPTLC plate together with a raftiline (RNE), raftilose (RSE) reference samples, and a mix of standard compounds. The agave samples of both species and all ages were randomly applied on the three chromatographic plates used per derivatizing agent. Finally, a pool of all samples was applied at the right end of each plate as a quality control sample (QC). The chromatographic elution consisted of a bi-ascendant separation; the first mobile phase was a mixture of isopropanol-butanol-water-acetic acid (14:10:4:2, v/v/v/v). The second mobile phase consisted of a mixture of isopropanol-butanol-water-acetic acid-formic acid (14:10:4:1:1, v/v/v/v/v). Saturation time of the chamber was 20 min for each development. For the first chromatographic separation the solvent migration distance was 75 mm measured from the application point and 85 mm for the second one. The drying time of the development solvent mixture was set to 5 min inside the development chamber drying compartment. For bands' visualization, the developed HPTLC plates were derivatized by immersion in aniline, α-naphthol, and orcinol. The HPTLC plates were heated in an oven at 120 °C for 3 min for aniline and 110 °C for the other two reagents. For plate derivatization, all the derivatizing reagents were freshly prepared. Images of the plates were recorded using a TLC visualizer under white R/T light after derivatization with 55 ms as exposition time.

2.5. Derivatizing reagent preparation

Diphenylamine-aniline-phosphoric acid. 50 mL of diphenylamine [4%] in acetone with 50 mL of aniline [4%] in acetone were mixed. Subsequently, 10 mL of phosphoric acid were added to the mixture under continuous stirring until a clear light brownish solution was formed. *α-Naphthol.* 2 g of α-naphthol were dissolved in 180 mL of absolute ethanol and 12 mL of sulfuric acid [50%] in ethanol was added to the mixture. A light pink solution was formed. *Orcinol.* 250 mg of orcinol were dissolved in 95 mL of absolute ethanol. Finally, 5 mL of sulfuric acid were added to the mixture and a clear colorless solution was formed.

2.6. Standard compounds and reference samples

Glucose, fructose, and sucrose were obtained from Sigma-Aldrich (St. Louis, Missouri); 1-kestose, 1-nystose, and 1-F fructofuranosylnystose (DP5) were obtained from Wako Pure Chemical Industries (Osaka, Japan). All standard compounds were ≥99.50% pure. Sample references Raftilose (RSE) and Raftiline (RNE) were purchased from Beneo-Orafti (Tienen, Belguim).

2.7. Data extraction and analysis

A negative filter was applied on-line (https://invert.imageonline.co/es/) to HPTLC pictures before data extraction. Subsequently, HPTLC data was extracted using rTLC (version 1.0) software (Fichou et al., 2016). For data bucketing, a pixel width of 128 pixels was used. Data from the RGB and gray channels were obtained for all the samples and derivatizing reagents. After data processing, all signals were normalized to the corresponding pooled QC signals in each chromatographic plate. The normalized data was used for multivariate data analysis (MVDA). As the main band information was observed from R_f 0.02–0.70, only data from this area was used for MVDA, that is 69 buckets/variables for each sample. Data was also scrutinized for reversal profile with GelAnalyzer (V.19.1).

The data was firstly scrutinized by principal component analysis (PCA) using the unit variance (UV) and pareto scaling methods. Data was also modeled by orthogonal projection to latent structures discriminant analysis (OPLS-DA) using the pareto scaling method to individually look on species and age effects. The correlated variables to each class were determined in a S-Plot with p(corr)-value equal or higher than 0.40 (Ivanović et al., 2021). A correlation between the age of the samples and their metabolic variation was explored through an orthogonal projection to latent structures (OPLS) analysis using the UV scaling method. The correlated variables were selected by their values in the predictive variable importance for the projection (VIP_{pred})-plot, that is > 1. The OLPS-DA and OPLS analyses were validated by cross-validation in a CV-ANOVA test ($p \leq 0.05$) and their prediction power was validated by permutation test (100 permutations) ($Q^2 \geq 0.40$).

Soft independent model of class analogy (SIMCA) analysis was performed using agave age as PCA classes scaled by UV method. In this model local PCAs were constructed for each age and the distances to the model (DmodX) were calculated and used to determine the similarity between technical replicates of samples of the same age. DmodX values were averaged ($n = 5$) and their standard errors were taken as measurement of their variation (Salomé-Abarca et al., 2021). All analysis were performed using SIMCA P (version 17.0.1, Umetrics, Umeå, Sweden).

3. Results and discussion

3.1. Fructooligosaccharides fingerprinting by HPAEC-PAD

The visual inspection of the HPAEC chromatograms of *Agave potatorum* and *Agave angustifolia* did not show evident qualitative differences between species. Conversely, the chromatograms showed clear quantitative differences, especially on simple sugars. That is, a clear lower content of glucose, fructose, and sucrose was observed in older specimens of both *Agave* species. Moreover, the apparition of higher-DP chromatographic peaks was observed in older specimens of both *Agave*

species (Fig. S1). This was more evident in *A. potatorum* specimens. For instance, the chromatogram of a one-year-old specimen show little or no presence of DP-8 to DP-12 agavin fructooligosaccharide (aFOS) when compared to that of six-years-old. Furthermore, both species showed a high degree of isomers as the polymerization degree (DP) increased in the chromatogram (Fig. S1). The maximum DP observed in both species was DP-12. This is caused by the ethanolic precipitation of higher-DP fructans. This can be corroborated by the HPAEC chromatogram of raftiline also subjected to alcohol precipitation. The degree of polymerization was also corroborated with a mixture of standard compounds (Fig. S1).

Nonetheless, the multivariate data analysis of aFOS from *A. potatorum* and *A. angustifolia* showed a clear separation by principal component analysis (PCA), mainly dictated by species factors, either scaled by pareto or unit variance (UV) (Fig. 1A and B). The PCA model scaled by pareto yielded a model with 4 PCs, which explained 66% of the total variation of the model ($RX^2cum = 0.66$). This model clustered samples according to species along the PC1 (34%), and according to age along the PC2 (12%) (Fig. 1C). On the other hand, Scaling by UV produced a model with 4 principal components (PCs) which explained 32% of the total variation of the model ($RX^2cum = 0.32$). The species' cluster separation was observed along the PC1 which captured 11% of the total variation of the model. PC2, which explained 8% of the total variation, showed sample separation by age (Fig. 1D). To eliminate species effects, the sample set was separated in individual species and analyzed by PCA. Both models, *A. angustifolia* and *A. potatorum*, showed sample separation according to age in both PC1 and PC2. Interestingly, the score plot showed an aggrupation of samples from one-to three-years-old, and from four-to six-years-old. However, this aggrupation is clearer in *A. angustifolia* samples, which indicates a stronger effect of age on its aFOS composition and accumulation over time (Fig. 1E and F).

Species effects were further scrutinized by orthogonal projection to latent structures discriminant analysis (OPLS-DA). The model included two classes, *A. potatorum* and *A. angustifolia*, and it was scaled by pareto.

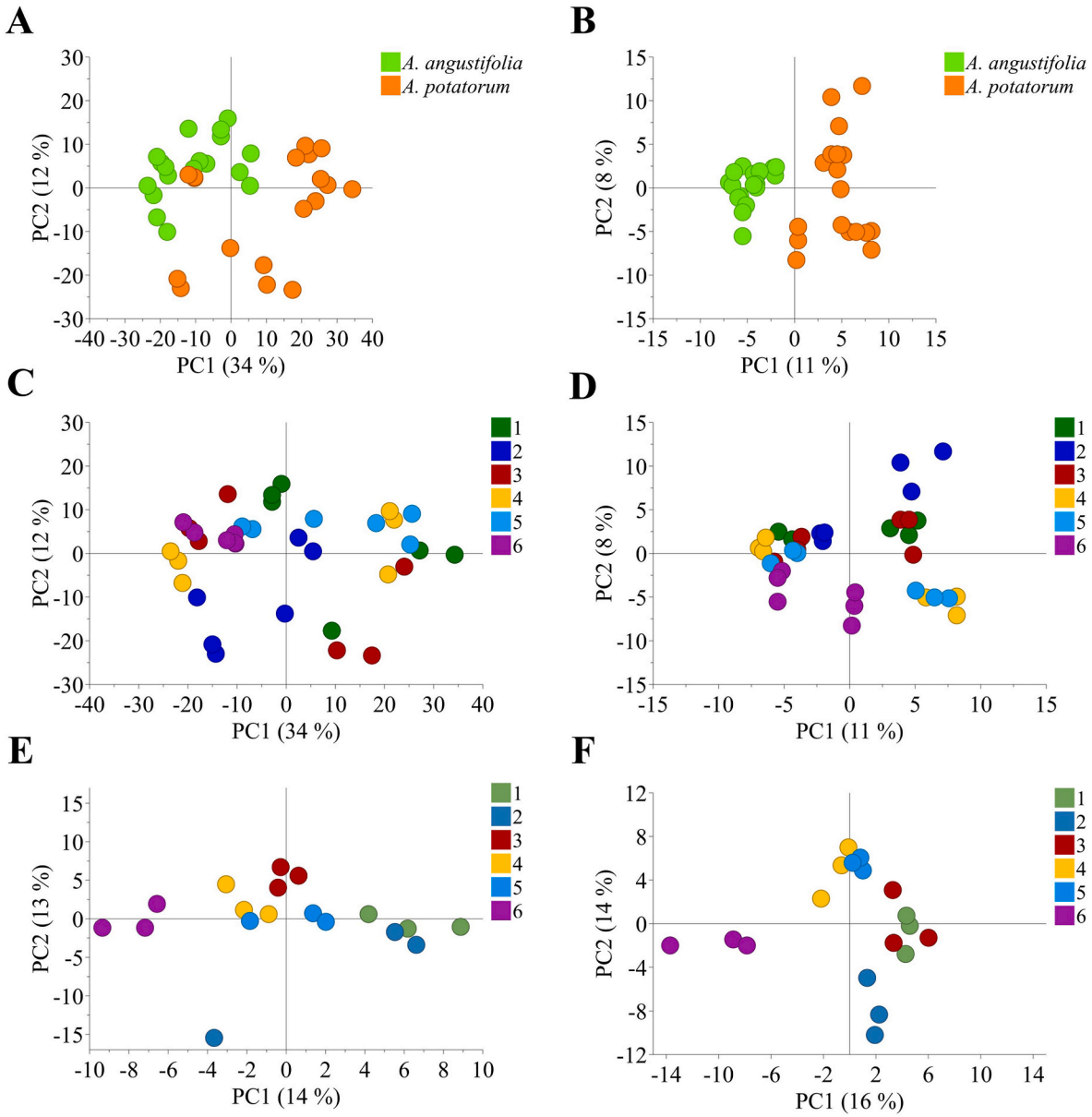

Fig. 1. Unsupervised multivariate data analysis of fructooligosaccharide fractions of *Agave angustifolia* and *Agave potatorum* measured by high performance anion Exchange chromatography. **A,** Principal component analysis (PCA) scaled by Pareto and colored according to Agave species. **B,** PCA scaled by unit variance (UV) and colored according to Agave species. **C,** PCA scaled by Pareto and colored according to Agave age. **D,** PCA scaled by UV and colored according to Agave age. **E,** PCA of *A. angustifolia* specimens scaled by pareto and colored according to age. **F,** PCA of *A. potatorum* specimens scaled by pareto and colored according to age.

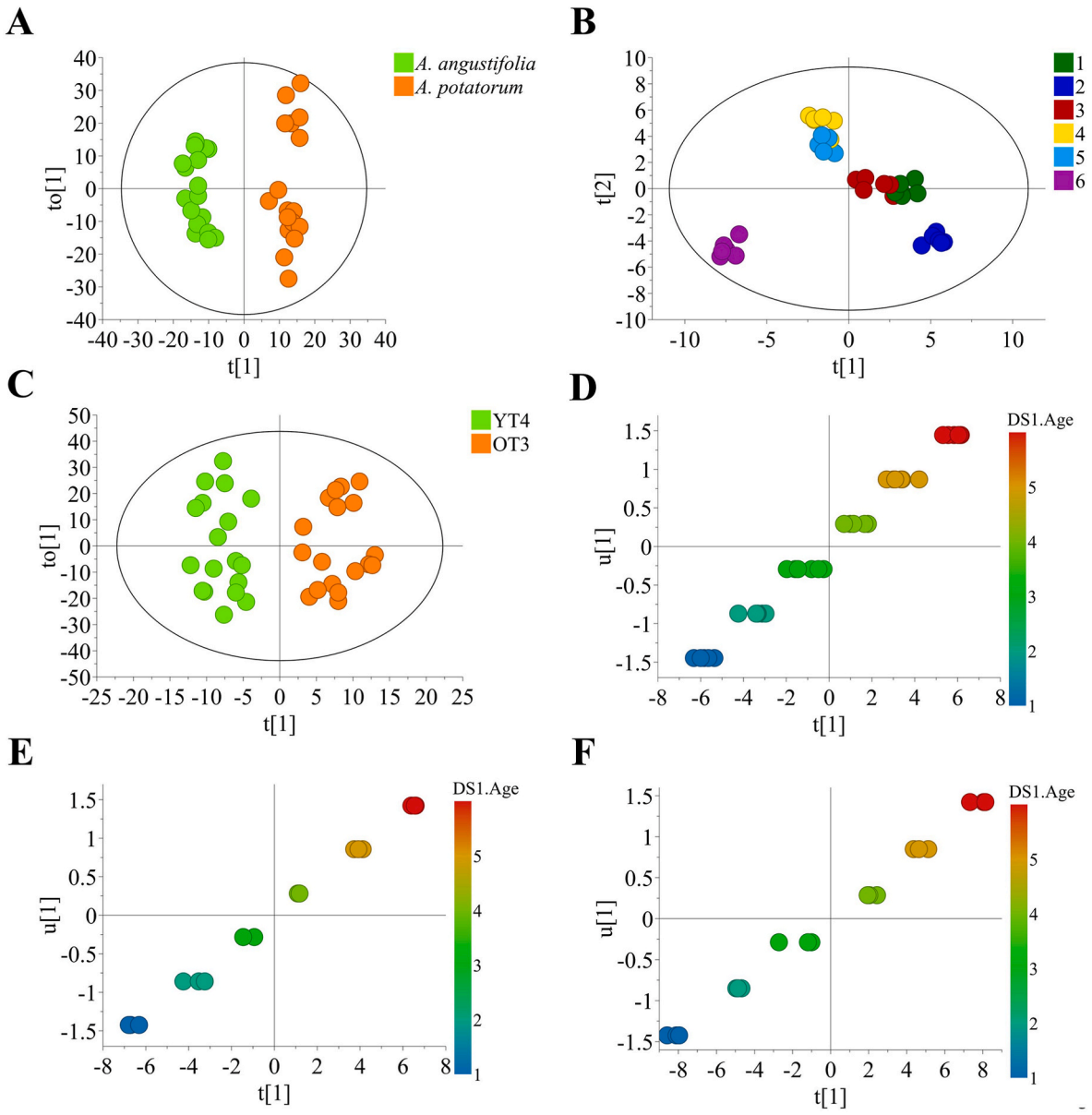

Fig. 2. Supervised multivariate data analysis of fructooligosaccharide fractions of *Agave angustifolia* and *Agave potatorum* measured by high performance anion Exchange chromatography. **A,** Orthogonal projection to latent structures discriminant analysis (OPLSDA) scaled by pareto and classified according to Agave species. **B,** OPLS-DA scaled by unit variance (UV) and classified according to Agave species. **C,** OPLS-DA scaled by pareto and classified according to binary age; YT4, specimens younger than four years and OT3, specimens older than three years. **D,** Orthogonal projection to latent structures (OPLS) by UV including all Agave samples. **E,** (OPLS) by UV including only *A. angustifolia* samples. **F,** (OPLS) by UV including only *A. potatorum* samples.

The analysis showed a clear separation of the sample set (Fig. 2A) and good validation with $Q^2 = 0.92$ and $p = 1.55 \times 10^{-14}$ in the permutation and CV-ANOVA test, respectively. The S-plot of the model showed characteristic higher contents of glucose (7.50 min), fructose (8.25 min), and isoforms of 1-F fructofuranosylnystose (DP-5) (21.36 and 22.06 min) in *A. potatorum*, while higher contents of sucrose (10.20 min) and DP-7 isoforms (30.41 and 31.71 min) were more representative of *A. angustifolia* specimens (Fig. S2). The confirmation of species effects on the agave samples indicates a differentiation on primary metabolism among them. For instance, the major content of sucrose in *A. angustifolia* might indicate a higher activity or a positive allosteric regulation of sucrose 6-phosphate synthase and sucrose phosphatase (Chua et al., 2008; Hawker and Hatch, 1966). Furthermore, differences in characteristic DPs of aFOS also indicates enzymatic differences in at least 1-fructosyltransferase (1-SST) and sucrose:fructan 6-Fructosyltransferase (6-SFT), responsible for inulin (β (2 → 1) chain elongation (Kawakami and Yoshida, 2002), and levan (branching, β (2 → 6) formation (Duchateau et al., 1995), respectively. In the case of 6G-fructosyltransferase (6G-FFT), even if HPAEC is capable to differentiate between F-series and *neo*-series in inulin like fructans (Ritsema et al., 2003), this is difficult or impossible to achieve for aFOS, where several peaks, many times overlapped, can be produced for a single DP (Mellado-Mojica and López, 2012; Huazano-García and López, 2018; Aldrete-Herrera et al., 2019). Thus, HPAEC cannot directly confirm the activity of this enzyme.

When performing orthogonal projection to latent structures discriminant analysis (OPLS-DA) using age as classes the models were not well validated. However, an OPLS-DA model scaled by UV using all samples classified by age produced a model with $Q^2 = 0.62$ and $p = 0.13$ (Fig. 2B). Even if the *p*-value of this model was not significant, it indicated a trend in the data (Salomé-Abarca et al., 2018). Interestingly, the OPLS-DA plot also showed an aggrupation of samples from one-to

three-years-old to the right side of the plot and samples from four-to six-years-old to the left side of the plot (Fig. 2B). This suggested a metabolic differentiation occurred between three- and four-years-old specimens. Thus, samples were classified as younger than 4 years (YT4) and samples older than three years (OT3) and analyzed by OPLS-DA. The model showed a good separation (Fig. 2C), and it was well validated ($Q^2 = 0.66$, $p = 8.13 \times 10^{-15}$). The S-plot of the analysis showed that YT4 specimens contained higher amounts of fructose (8.25 min) and sucrose (10.19 min) than older specimens (Fig. S2), which indicates that simpler carbohydrates may serve as building blocks for the synthesis of higher-DP fructans (Mellado-Mojica and López, 2012). In agreement with this data, OT3 specimens were characterized for containing higher amounts of DP-6 (25.66 and 27.08 min), DP-7 (31.15 and 32.77 min), DP-8 (36.85 min), and DP-9 (44.94 min). Therefore, a tendency of simpler sugars consumption for producing higher-DP aFOS through time was stablished.

To get more insight in the production and accumulation trend of aFOS in relation with age, the age of *Agave* specimens was used as quantitative data classified as "Y" variable in an orthogonal projection to latent structures (OPLS) analysis. The model looked for a potential linear correlation between age increase and aFOS variation. First, a model using all agave samples was constructed showing a positive linear correlation between age increase and aFOS accumulation (Fig. 2D). That is, the DP and content of aFOS increase as the agave age increases ($Q^2 = 0.80$, $p = 8.13 \times 10^{-5}$). Interestingly, when the sample set was divided in individual species, a differential degree of correlation was observed in *A. potatorum* and *A. angustifolia*. For instance, a $Q^2 = 0.82$ and 0.76 were determined for *A. potatorum* and *A. angustifolia* in their individual OPLS analyses (Fig. 2E and F). Moreover, $p = 9.33 \times 10^{-5}$ and 0.006 were determined in the CV-ANOVA test of each OPLS model. A similar trend was observed when the relative amount of fructans up to DP-16 were used as variables and plotted in a heat map. For instance, a clear accumulation pattern of high-DP fructans and reduction of simpler carbohydrates was observed as the agave age increased (Márquez-López et al., 2022). The same trend was proposed for *Agave tequilana* var. azul. This species exhibited changes in carbohydrate, total fructan content, DP, type, and molecular structure through time in the field (Mellado-Mojica and López, 2012), which is in accordance with the observed results. Therefore, up to this point, HPAEC-based chemometrics has been able to determine carbohydrate and aFOS differences associated to species effects and correlations with age increase at the field.

3.2. *Fructooligosaccharides fingerprinting by high performance thin layer chromatography (HPTLC)*

Even if HPAEC was proven as a robust chemometrics-based platform, it possesses some disadvantages, especially a long-time analysis. Analyses through this technique imply around 45–75 min per fructan sample, which would result in large analysis periods for large sample sets. In the context, HPTLC analysis offers the possibility of parallel sample analysis, and it has been proven as a good supplementary analytical platform for the fingerprinting of several specialized metabolites. Nonetheless, there are several factors that determine the data quality acquired by this technique. Some of them are the mobile phase and the choice of the proper derivatizing reagent (Komsta, 2012; Fichou et al., 2016). Moreover, the combination of derivatizing reagents with adequate chromatographic plate illumination, before and after derivatization determine the general or selective detection character of the metabolite analysis (Ristivojević et al., 2014).

However, in this study, the sample extraction method resulted in a target analysis. That is, a carbohydrate fraction and agavin-fructooligosaccharides (aFOS) were obtained from the fructan samples, which delimited the options to choose derivatizing reagents. In this regard, diphenylamine-aniline-phosphoric acid (referred as aniline) is considered one of the most useful derivatizing reagents for fructans detection on TLC (Reiffová and Nemcová, 2006). Even its detection sensitivity, given by color, is much higher than those of refraction index and evaporative light scattering detectors, which are common detectors for HPLC (Morlock and Sabir, 2011; Li et al., 2013; Zhao et al., 2017). Nonetheless, α-naphthol was found to be more sensitive for fructans detection when compared to aniline on HPTLC analysis (Benkeblia, 2013). Lastly, orcinol is also frequently used for fructan and levan like metabolites detection on regular TLC (Aramsangtienchai et al., 2020; Madia et al., 2021). These features settled the election of these three reagents as derivatizing reagents for this study. Finally, the lack of inherent color or fluorescence of carbohydrates delimited the plate illumination to white light after derivatization.

In this study, the visual inspection of the HPTLC chromatograms, showed differential patterns between *Agave* species and ages. Such differences were clearly visible independently of the derivatizing reagent used to dye the plates. The main differences were observed at the retention factor (R_f) range of 0.01–0.60 (Fig. 3A). In general, meanwhile α-naphthol and orcinol showed strong single-color patterns (Fig. 3B and C), aniline showed lighter chromatographic spots. Nonetheless, aniline produced bicolor patterns, that is, when fructans are separated by HPTLC and derivatized with this reagent, glucose bearing structures developed blue color on the plate (Fig. 3A). This indicated that glucose was added to such fructan. Since 6G-FFT is the enzyme responsible for such task (Ritsema et al., 2003), the activity of this enzyme can be demonstrated by the detection of its products. On the other hand, fructans without glucose in their structures developed pink color, such fructans are denominated the F-series because they are composed of only fructose. Furthermore, the maximum visually countable degree of polymerization of *Agave* samples determined by HPTLC was DP-11. This DP was determined by counting the number of chromatographic spots from top to bottom taking as starting reference the band of 1-kestose as DP-3 (Fig. 3A and S3).

So far, this is the maximum information that have been obtained from regular TLC visual analysis of agave-fructan samples (Mellado-Mojica and López, 2012; Alvarado et al., 2014; Pérez-López et al., 2021). However, the automation of TLC and the development of specialized software for HPTLC data allows for several image and data treatment such as image reconstruction, pixel extraction, band warping, among others (Fichou et al., 2016). Additionally, HPTLC data produces four different data bases in the so called RGB channels, which correspond to densitograms in the red, green, and blue color plus a fourth scale denominated the gray channel. The gray channel is an average of the intensities of the RGB channels (Fichou et al., 2016). This data treatment has allowed for the successfully implementation of multivariate data analysis to HPTLC data of biological samples such as propolis, pine resins, *Cistus* samples, among others (Morlock et al., 2014; Salomé-Abarca et al., 2018, 2020). Surprisingly, due to the darkish color of bands and lighter background of the plate, the intensity values of the chromatographic plates were inverted during the data extraction. That is, strong colored bands produced lower or negative intensity peaks, while light colored spots produced higher intensity peaks in the HPTLC densitograms (Fig. S4). This fact was corroborated with the software GelAnalyzer, which is capable to separately analyze lighter bands in dark background and darker bands in lighter background. Unfortunately, rTLC does not possesses this feature, and GelAnalyzer does not perform bucketing. Thus, a solution for this issue was to invert the color of HPTLC images by applying a negative filter. This resulted in the same densitogram pattern as that of dark on light background (Fig. S4). Thus, negative HPTLC images were submitted to rTLC to get data of agave FOS from *Agave angustifolia* and *Agave potatorum*, which yielded all the previously mentioned data sets per each derivatizing reagent used in this study (Figs. S5 and S6).

The chromatographic data showed neglectable Rf shift, thus, warping algorithm was no applied to the data set. This was observed when overlapping densitograms of quality control (QC) samples applied at the same position in all chromatographic plates (Fig. S7). For instance, when overlapping QC samples of plates derivatized with α-naphthol, they

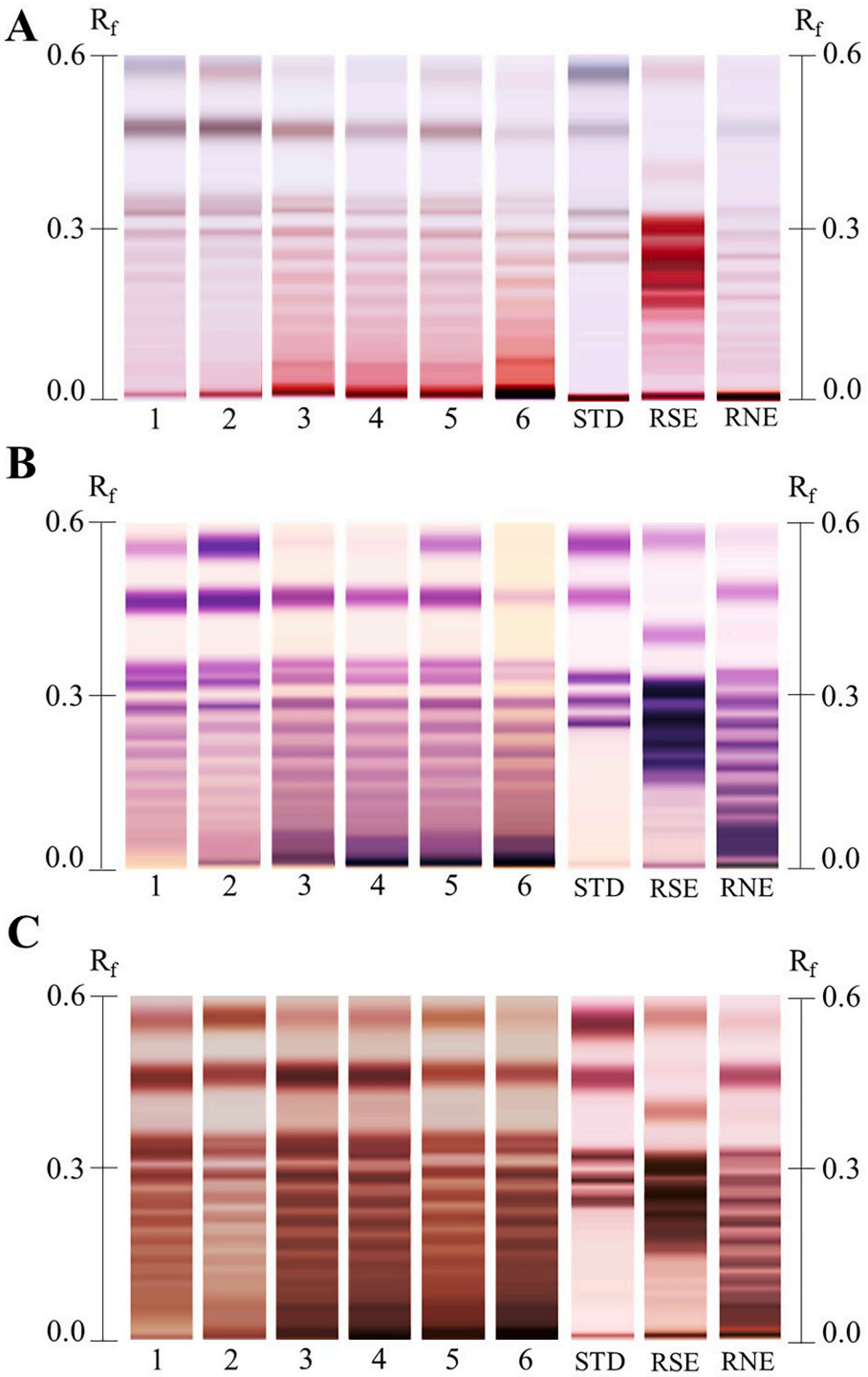

Fig. 3. HPTLC chromatograms of representative *Agave angustifolia* samples derivatized with **A,** aniline, **B,** α-naphthol, and **C,** orcinol. Sample number corresponds to sample age measured in years. STD corresponds to a standard compound mixture containing fructose/glucose, sucrose, 1-kestose, 1-nystose, and 1-F fructofuranosylnystose (DP-5) [2 mg/mL]. They appear from top to bottom in the mentioned order. RSE and RNE correspond to commercial samples of raftilose and raftiline, respectively.

showed almost a perfect overlap and small differences might be caused by technical variations at the HPTLC system (Fig. S7A). However, this cross-plate variation is fixed when normalizing samples' intensity to the intensity of each QC sample in the corresponding HPTLC plate (Salomé-Abarca et al., 2018). Moreover, the despicability of Rf shift was observed when overlapping densitograms of the QC samples of the first plate used with each derivatizing reagent (Fig. S7B).

To assess the reproducibility (variation) of the sample preparation method for fingerprinting purposes, three agave samples of one, three and five years-old were selected. The samples were prepared as described in methods and individually spotted and separated by HPTLC. The data was extracted as previously described and the gray channel was used to scrutinize the variation among samples. To do so, a soft independent model of class analogy (SIMCA) analysis was performed using the agave age as PCA classes (Salomé-Abarca et al., 2021). In this model, local PCAs are separately constructed for each class (age) and the distances to the model (DModX) are calculated. The model uses the critical value of DModX, so called Dcrit, to determine similarity between samples and classes, a measurement of variation. Thus, any sample with value above the Dcrit line are considered different from the set class. Thus, samples of the same class shall be all under the Dcrit line (Eriksson et al., 2011). Therefore, the SIMCA analyses of each age demonstrated

that the effect of sample preparation did not cause large variation on technical replicates (Fig. S8). Furthermore, the DmodX of each selected agave sample were determined, averaged and their standard errors were calculated. The DmodX values for samples of one, three, and five years-old were 0.98 ± 0.08, 0.99 ± 0.05, and 0.99 ± 0.05, respectively. These values represented 8 and 5% of variation among technical replicates.

Subsequently, the data was firstly approached by PCA. Considering three derivatizing reagents, four color channels, and two scaling methods (UV and Par), a total of 24 PCA models were scrutinized. All models showed two main clusters separated along the PC1, which corresponded to *Agave* species (Fig. 4A and B). In the same manner as HPAEC data, the plots from HPTLC data always showed better separation when pareto scaling was used to build the models. When PCA models were colored by age, all of them showed sample separation according to this factor in each species cluster along the PC1 and PC2 (Fig. 4C and D). Moreover, every single plot showed that the six-years-old samples from *A. potatorum* were clustering closer to the six-years-old samples of *A. angustifolia*. This could be explained by the marked visual increase of higher DP-aFOS as the agave age increases, thus, HPTLC patterns of older specimens become more similar between them causing their clustering. This can be appreciated when comparing the chromatogram patterns of the six-years-old samples of both species (Fig. 3 and S3). These phenomena have also been observed in plants of *Agave tequilana* Weber var azul grown under field conditions (Aldrete--Herrera et al., 2019).

However, the PCA model produced from samples derivatized with aniline and extracted in the gray channel was able to better separate samples by *Agave* species and better differentiate the six-years-old samples of *A. potatorum* and *A. angustifolia* (Fig. 4A and B). This model explained 90% of the total variation of the model ($R^2Xcum = 0.90$) and produced six principal components (PCs). This means that the PCA generated from this channel explained almost 30% more variation in the model than that of HPAEC data. This means that only 10% of the

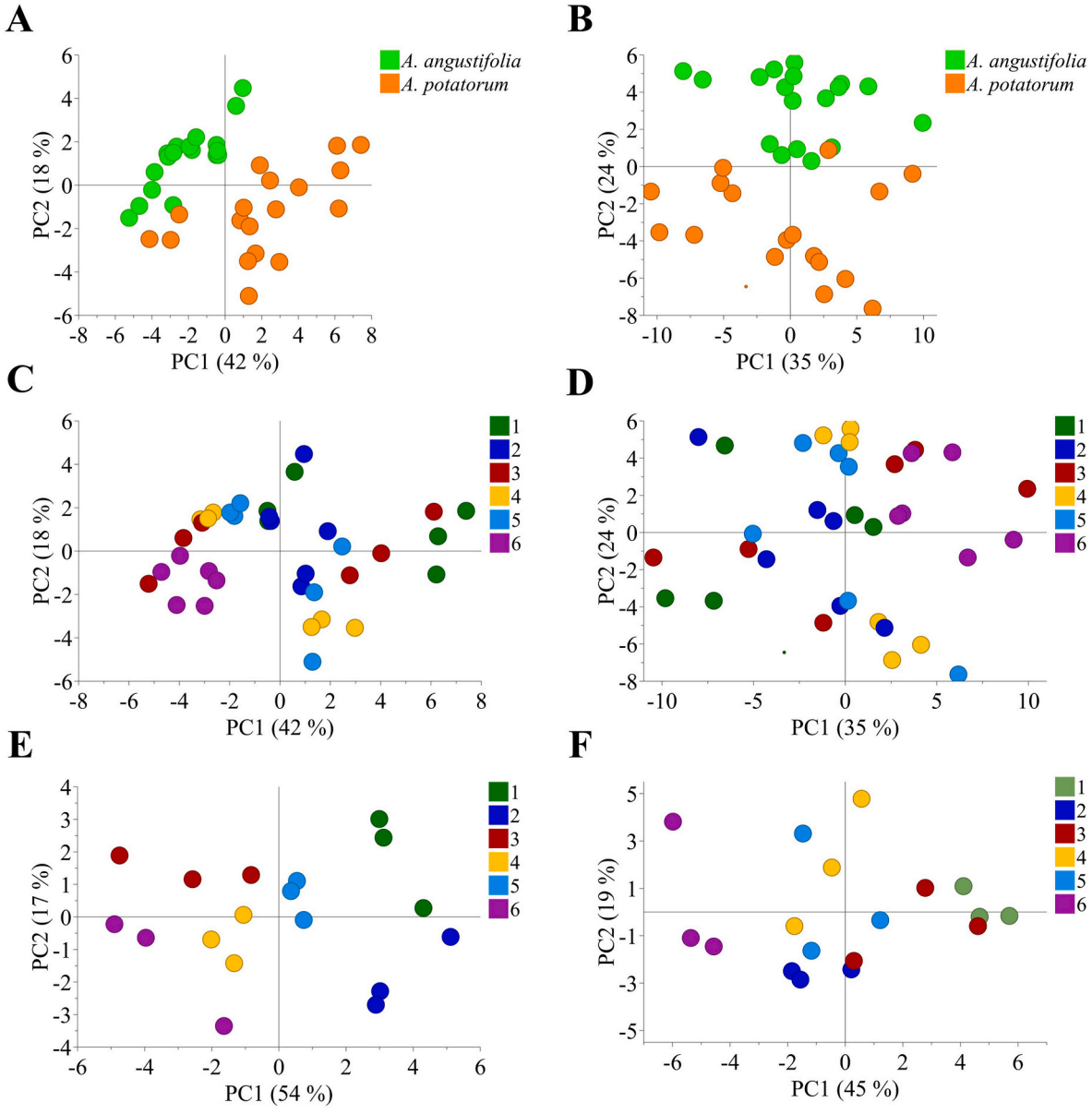

Fig. 4. Unsupervised multivariate data analysis of fructooligosaccharide fractions of *Agave angustifolia* and *Agave potatorum* measured by high performance thin layer chromatography. **A,** Principal component analysis (PCA) scaled by pareto and colored according to Agave species. **B,** PCA scaled by unit variance (UV) and colored according to Agave species. **C,** PCA scaled by pareto and colored according to Agave age. **D,** PCA scaled by UV and colored according to Agave age. **E,** PCA of *A. angustifolia* specimens scaled by pareto and colored according to age. **F,** PCA of *A. potatorum* specimens scaled by pareto and colored according to age.

variation of the model was not explained by carbohydrate and aFOS data. The PC1 captured 40% of the variation of the model, and the PC2 captured around 19% of the total variation. Thus, only 2 PCs obtained from HPTLC data explained around the same variation explained by 4 PCs obtained from HPAEC data. To eliminate species effects over the plot separation, the sample set was divided by species and individually analyzed. The best PCA models separating samples according to age were also those produced from aniline extracted from the gray channel for *A. potatorum* and *A. angustifolia* (Fig. 4E and F).

Following the same MVDA approach, the sample set was modeled by means of OPLS-DA. In this model, two classes were set (*A. potatorum* and *A. angustifolia*) and scaled by pareto. In general, all models from all derivatizing reagents and color channels were able to separate samples by species. However, the model with the best visual separation and the highest Q^2-value ($Q^2 = 0.82$) was the one produced by plates derivatized with α-naphthol extracted in the green channel (Fig. 5A). The model was also well validated by the CV-ANOVA test with $p = 2.39 \times 10^{-8}$. The S-plot of the model showed that a higher content of glucose/fructose (R_f 0.566) and DP5 (R_f 0.253–0.264) is representative of *A. potatorum* specimens (Fig. 3B). In the case of *A. angustifolia*, a higher content of sucrose (R_f 0.465) and higher-DP aFOS (R_f 0.041–0.132) is more representative of this species (Fig. S9). Contrastingly, all OPLS-DA models attempting to separate samples according to age failed to achieve a cluster separation ($Q^2 < 0.40$, $p > 0.05$). This might be due to the lack of enough differentiation features detected by HPTLC between each analyzed age.

In the context, the PCA analyzes of individual species showed that three- and four-years-old samples were similar between each other in *A. angustifolia* (Fig. 4E and F). On the other hand, four-years-old samples tended to be more similarly to five-years-old samples in *A. potatorum*, which means they possess similar HPTLC patterns, that is, aFOS composition. Thus, the analyses showed a special metabolic

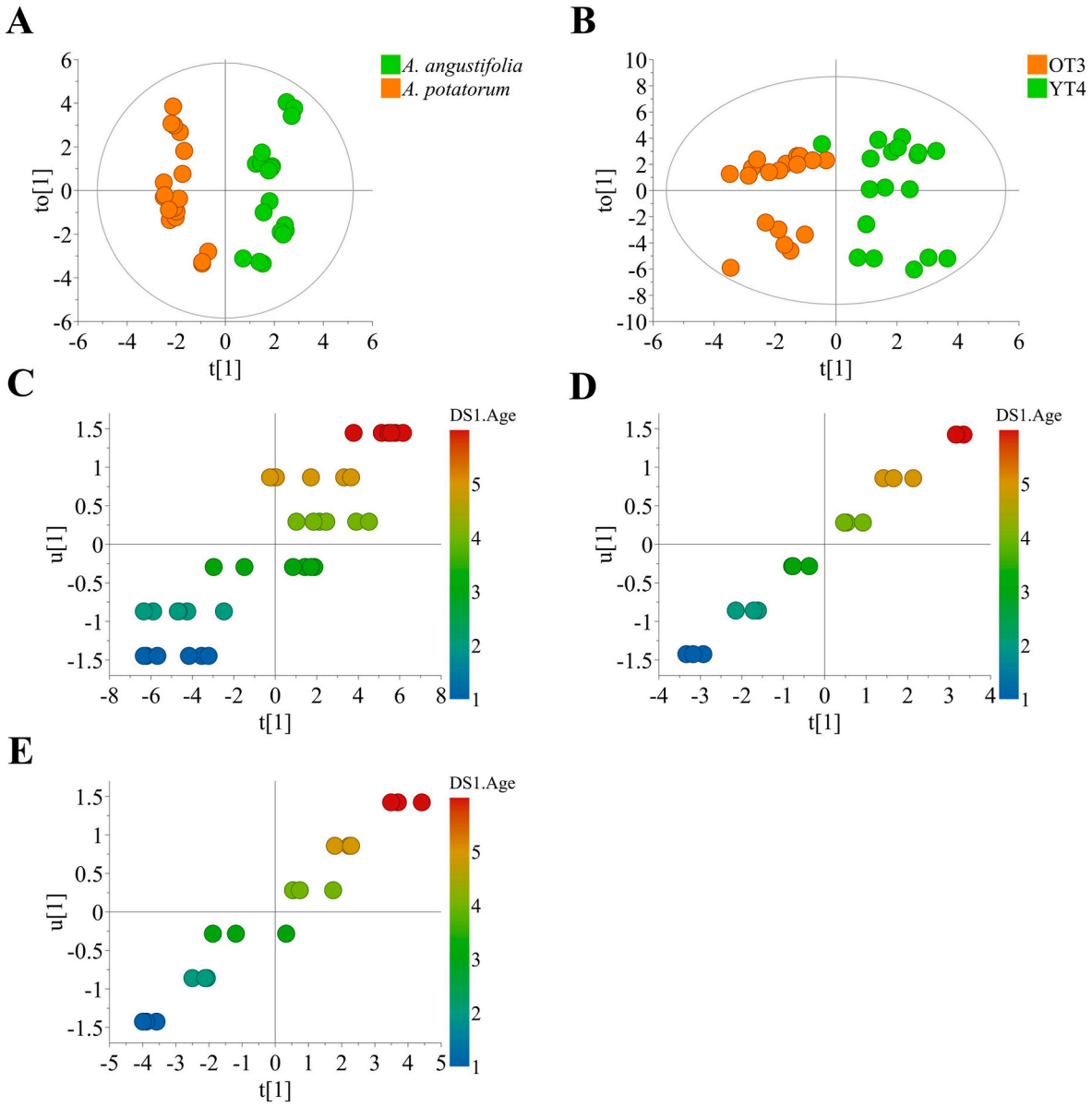

Fig. 5. Supervised multivariate data analysis of fructooligosaccharide fractions of *Agave angustifolia* and *Agave potatorum* measured by high performance thin layer chromatography. **A,** Orthogonal projection to latent structures discriminant analysis (OPLS-DA) scaled by pareto and classified according to Agave species. **B,** OPLS-DA scaled by pareto and classified according to binary age; YT4, specimens younger than four years and OT3, specimens older than three years. **C,** Orthogonal projection to latent structures (OPLS) by UV including all Agave samples. **D,** (OPLS) by UV including only *A. angustifolia* samples. E, (OPLS) by UV including only *A. potatorum* samples.

differentiation between three- and four-years-old onwards in agave samples as previously suggested by HPAEC. Therefore, a new OPLS-DA model with two classes, samples younger than four-years-old (YT4), and samples older than three-years-old (OT3) was performed to scrutinize age effects.

Most of the models successfully separated YT4 and OT3 samples ($Q^2 > 0.40$, $p < 0.05$) (Table S1). The model uncapable to separate agaves samples according to this classification was that resulted from aniline extracted in the green channel. This model did not show enough predictive power ($Q^2 = 0.30$), but it showed a significant effect of age in the model ($p = 0.02$). However, the best model for separating samples classified by binary age was that produced from samples derivatized with aniline extracted from the blue channel ($Q^2 = 0.61$, $p = 0.002$) (Fig. 5B). Thus, the effect of age on the aFOS fraction of *A. potatorum* and *A. angustifolia* was confirmed by both analytical platforms. The S-plot of the model indicated that YT4 samples possessed higher amounts of glucose, fructose (R_f 0.516–0.556), sucrose (R_f 0.425–0.476), 1-kestose, and *neo*-kestose (R_f 0.340–0.385). Conversely, OT3 samples presented higher content of DP-6 to DP-11 aFOS (R_f 0.021–0.213) (Fig. S9). This means there is a decrease of simpler sugars and increase of higher-DP fructans as the age of agave increase, probably because simple sugars are used as substrate to synthesize higher-DP fructans (Mellado-Mojica and López, 2012). This data match with the results found by HPAEC analysis.

Continuing with the scrutiny of age affects, orthogonal projection to latent structures (OPLS) models were constructed to determine if HPTLC also determines linear correlations between the increase of *Agave* age and their metabolic variation. First, all HPTLC data from *A. potatorum* and *A. angustifolia* samples were used together as X variables and the corresponding age of each sample was set as quantitative Y-variable in the model. The same approach was used in two OPLS models using only *A. potatorum* or *A. angustifolia* samples. All models, all the derivatizing reagents and color channels demonstrated a linear correlation between the sample age increase and their metabolic variation (Table S1). The best OPLS models were those resulted from α-naphthol in the in the green channel for all-agave samples ($Q^2 = 0.98$, $p = 2.93 \times 10^{-7}$), and orcinol in the red channel for *A. angustifolia* ($Q^2 = 0.96$, $p = 1.00 \times 10^{-4}$) and *A. potatorum* ($Q^2 = 0.88$, $p = 0.002$) (Fig. 5C, D, and 5E). It is worth to highlight that HPTLC data produced OPLS models with higher Q^2-values than those of HPAEC data. Thus, the OPLS models produced from HPTLC data possess good potential for prediction of aFOS content according to agave age.

The most correlated variables with the age increase in the agave aFOS were determined according to the predictive variable importance for the projection (VIP_{pred})-plot. In this plot, all variables with VIP-values equal or higher than one are considered important for the model projection (Ivanović et al., 2021). The R_f values correlated to the increase of age in the all-agave samples model were high-DP aFOS but specially DP-7, DP8, and D-P9 (R_f 0.142, 0.132, 0.112, 0.163, 0.173, 0.183, and 0.102). In the case of *A. potatorum*, the model indicated that DP10 and DP11 (R_f 0.041–0.092), the R_f range 0.102–0.173 (also observed in the all-samples model), DP6 (R_f 0.203), are correlated to the increase of age in this species. For *A. angustifolia* samples, the range R_f 0.021–0.072 was strongly correlated to the increase of age in this species; such range might correspond to unresolved DP-12. Furthermore, an increase of nystose (R_f 0.294) and DP-9 (R_f 0.132) was also correlated to the age increase in *A. angustifolia*. Moreover, it is worth noting that the R_f range 0.041–0.193 was the range with the highest VIP_{pred} values in the three models (Fig. 5C, D, and 5E), which means that an increase in the production and accumulation of higher-DP fructans is linearly correlated to the increase of the age of *A. potatorum* and *A. angustifolia* specimens.

Up to this point, orcinol produced the models with the highest predictive power (Q^2) and the most significant *p*-values and α-naphthol the ones with lowest Q^2 and *p*-values (Table S1). Nonetheless, aniline models were also able to discriminate samples by species, age, and it provided visual information about isomers composition. For instance, while in regular TLC and HPLTC analysis derivatized with orcinol and α-naphthol, glucose and fructose appear as a single-broad spot, the HPTLC analysis of these components derivatized with aniline show a degree of separation between these sugars. That is, glucose appears as a bluish band with slightly higher R_f value than that of fructose, which appears as a pink band right under glucose (Fig. S3). Moreover, considering that the HPTLC data is extracted by making buckets of a selected pixel size (Fichou et al., 2016), the buckets corresponding to fructose or glucose can be discriminated, therefore, making possible to assign punctual and separated importance for these metabolites. In the context, the differential color produced by aniline derivatization is correlated to the type of glycosidic linkage present in the carbohydrate structure (Schwimmer and Bevenue, 1956; Kocourek et al., 1966). That is, glucose bearing aFOS will always produce blueish spots, while only fructose-based aFOS will be pink colored. Thus, isomeric differentiation between FOS and their F-series isomers can be achieved. Hence, probably these features made aniline a better data matrix to observe natural differences among *Agave* species in PCA. Even if a negative filter could produce a visual loss of binary color, the negative colors would vary according to their original ones, thus keeping at some degree the differential bicolor character of aniline. Finally, standard DP5, raftilose, and raftiline will confirm the observed DP in the FOS extracts (Fig. 3 and S3).

Regarding color channels, in general, every color channel got at least one of the best models for a given feature. However, gray channel did show the clearest natural variation given by species and age factors on PCA plots. Conversely, red channel produced the best supervised models for correlation between age increase and aFOS variation in individual models of *A. angustifolia* and *A. potatorum*. Contradictorily, aniline produced the best model for binary age extracted in the blue channel, and the worst non-validated model for the same feature but extracted in the green channel (Table S1). This denotes the importance of color channel extraction over the data quality (Table S1). Thus, in general, the channels with major number of the best models were as follows gray > red > green > blue and reagents aniline > α-naphthol = orcinol. Furthermore, this data demonstrates the importance of the combination of color patterns produced by derivatizing reagents and the color extracted from those patterns.

Similar facts have been observed in other natural product samples analyzed by HPTLC-based fingerprinting. Taken as example, the classification of Romanian medicinal plant extracts according to their therapeutic effects. In this study, the best image processing channels were identified for each of the investigated plates. Blue channel for HPTLC Silica gel 60 F_{254} was the best channel for PCA with 92.9% percent of discrimination (Simion et al., 2019). Another example is the rapid discrimination of different *Apiaceae* species based on their HPTLC fingerprints and targeted flavonoids (Shawky et al., 2018). In this research, also the blue channel separated almost all the species in the PCA analysis, and the not separated species were discriminated by the red and green channels. Thus, the obtained results suggested that different zones in each channel are responsible for such clustering, which might be the case of HPTLC analysis of agave samples.

A final important example is one dealing with the discrimination of propolis samples from different geographical origins (Germany, Romania, and Serbia). According to the HPTLC fingerprint analyses of propolis, two main types of European poplar-type propolis were determined, the so-called orange and blue propolis (Morlock et al., 2014; Milojković-Opsenica et al., 2016). As their names imply, the orange propolis, contains several strong orange chromatographic bands, few light blue, and faint green bands. Conversely, blue propolis shows typical deep and light blue bands, and feeble orange and green bands (Morlock et al., 2014). In this case, the red channel contributed to the densitogram intensity of orange bands, while blue channel was accounting more for blue bands. PCA was performed on the results obtained for each channel, and the best models were achieved with the red

channel data, probably due to the correlation of orange bands intensity with their geographical origin (Milojković-Opsenica et al., 2016). The inversion color effect of the negative filter, which results in one tone with different intensity patterns might indicate that differences among *Agave* species and ages might be more correlated to quantitative differences rather than qualitative ones, which is also suggested by HPTLC images.

4. Conclusions

aFOS profiles are robust enough to discriminate *Agave* species and describe carbohydrate metabolism through time either profiled by HPAEC or HPTLC. Thus, HPTLC-based fingerprinting is a good complementary or stand-alone platform for the characterization of fructooligosaccharides. Nonetheless, the type of derivatizing reagent and the extraction color channel determines the goodness of the model used to scrutinize the HPTLC data, that is predictive power (Q^2) and significance (p-values) of the model. Therefore, a good approach for the target profiling characterization of aFOS by HPTLC would be to use aniline for a general and unsupervised fingerprinting, then use either orcinol or α-naphthol for the creation of predictive models for specific variables. Finally, both HPAEC and HPTLC are sufficient to also provide information about specific (HPAEC) or general (HPTLC) isomer composition and their relation to fructooligosaccharides' metabolism in *Agave* species.

CRediT authorship contribution statement

Luis Francisco Salomé-Abarca: Conceptualization, Data curation, Formal analysis, Investigation, Methodology, Visualization, and, Writing – original draft. **Ruth Esperanza Márquez-López:** Investigation, Validation, Writing – review & editing. **Patricia Araceli Santiago-García:** Resources, Writing – review & editing. **Mercedes G. López:** Conceptualization, Supervision, Project administration, and, Writing – review & editing.

Declaration of competing interest

The authors declare that they have no known competing financial interests or personal relationships that could have appeared to influence the work reported in this paper.

Data availability

No data was used for the research described in the article.

Acknowledgments

We gratefully acknowledge the commercial producers: "Maestro Naxuhal" and "Mil Queridas" for providing plant material. The Research and Postgraduate Studies Secretariat (SIP) of the Instituto Politécnico Nacional (IPN-México) for their financial support (Projects 20221103 and PRO21DTIA). The second author thanks CONACYT for her Doctoral Fellowship (N° 788256). We also kindly acknowledge Prof. Dr. Jorge Molina Torres for providing access to the HPTLC system.

Appendix A. Supplementary data

Supplementary data to this article can be found online at https://doi.org/10.1016/j.crfs.2023.100451.

References

Aldrete-Herrera, P.I., López, M.G., Medina-Torres, L., Ragazzo-Sánchez, J.A., Calderón-Santoyo, M., González-Ávila, M., Ortiz-Basurto, R.I., 2019. Physicochemical composition and apparent degree of polymerization of fructans in five wild agave varieties: potential industrial use. Foods 8, 404. https://doi.org/10.3390/foods8090404.

Alvarado, C., Camacho, R.M., Cejas, R., Rodríguez, J.A., 2014. Profiling of commercial agave fructooligosaccharides using ultrafiltration and high-performance thin layer chromatography. Rev. Mex. Ing. Quim. 13, 417–427.

Aramsangtienchai, P., Kongmon, T., Pechroj, S., Srisook, K., 2020. Enhanced production and immunomodulatory activity of levan from the acetic acid bacterium *Tanticharoenia sakaeratensis*. Int. J. Biol. Macromol. 163, 574–581. https://doi.org/10.1016/j.ijbiomac.2020.07.001.

Arrizon, J., Hernández-Moedano, A., Oner, E.T., González-Avila, M., 2014. *In vitro* prebiotic activity of fructans with different fructosyl linkage for symbiotics elaboration. Int. J. Probiotics. 9, 69–76.

Arrizon, J., Morel, S., Gschaedler, A., Monsan, P., 2010. Comparison of the water-soluble carbohydrate composition and fructan structures of *Agave tequilana* plants of different ages. Food Chem. 122, 123–130. https://doi.org/10.1016/j.foodchem.2010.02.028.

Benkeblia, N., 2013. Fructooligosaccharides and fructans analysis in plants and food crops. J. Chromatogr. A 1313, 54–61. https://doi.org/10.1016/j.chroma.2013.08.013.

Cheong, K.L., Li, J., Zhao, J., Li, S.P., 2014. A simple analysis of fructooligosaccharides in two medicinal plants by high-performance thin-layer chromatography. J. Planar Chromatogr. 27, 245–250. https://doi.org/10.1556/jpc.27.2014.4.2.

Chua, T.K., Bujnicki, J.M., Tan, T.C., Huynh, F., Patel, B.K., Sivaraman, J., 2008. The structure of sucrose phosphate synthase from *Halothermothrix orenii* reveals its mechanism of action and binding mode. Plant Cell 20, 59–72. https://doi.org/10.1105/tpc.107.051193.

Cozzolino, D., Roumeliotis, S., Eglinton, J., 2014. Feasibility study on the use of attenuated total reflectance MIR spectroscopy to measure the fructan content in barley. Anal. Methods 6, 7710–7715. https://doi.org/10.1039/C4AY01560F.

Domínguez, A.L., Rodrigues, L.R., Lima, N.M., Teixeira, J.A., 2014. An overview of the recent developments on fructooligosaccharide production and applications. Food Bioprocess Technol. 7, 324–337. https://doi.org/10.1007/s11947-013-1221-6.

Duchateau, N., Bortlik, K., Simmen, U., Wiemken, A., Bancal, P., 1995. Sucrose:Fructan 6-fructosyltransferase, a key enzyme for diverting carbon from sucrose to fructan in barley leaves. Plant Physiol. 107, 1249–1255. https://doi.org/10.1104/pp.107.4.1249.

Eriksson, L., Byrne, T., Johansson, E., Trygg, J., Vikström, C., 2011. Process analytical technology (PAT) and quality by design (QbD). In: Eriksson, L., Byrne, T., Johansson, E., Trygg, J., Vikström, C. (Eds.), Multi- and Megavariate Data Analysis: Basic Principles and Applications, third ed. Umetrics Academy, Umeå, p. 500.

Fichou, D., Ristivojević, P., Morlock, G.E., 2016. Proof-of-principle of rTLC, an open-source software developed for image evaluation and multivariate analysis of planar chromatograms. Anal. Chem. 88, 12494–12501. https://doi.org/10.1021/acs.analchem.6b04017.

García-Villalba, W.G., Rodríguez-Herrera, R., Ochoa-Martínez, L.A., Rutiaga-Quiñones, O.M., Gallegos-Infante, J.A., González-Herrera, S.M., 2022. Agave fructans: a review of their technological functionality and extraction processes. J. Food Sci. Technol. 1–9. https://doi.org/10.1007/s13197-022-05375-7.

Gaudêncio, S.P., Pereira, F., 2015. Dereplication: racing to speed up the natural products discovery process. Nat. Prod. Rep. 32, 779–810. https://doi.org/10.1039/c4np00134f.

Ge, Y., Sun, M., Salomé-Abarca, L.F., Wang, M., Choi, Y.H., 2018. Investigation of species and environmental effects on rhubarb roots metabolome using 1H NMR combined with high-performance thin layer chromatography. Metabolomics 1–11. https://doi.org/10.1007/s11306-018-1421-1.

Gibson, G.R., Roberfroid, M.R., 2008. Handbook of Prebiotics, first ed. CRC Press, Boca Raton.

González-Herrera, S.M., Rutiaga-Quiñones, O.M., Aguilar, C.N., Ochoa-Martínez, L.A., Contreras-Esquivel, J.C., López, M.G., Rodríguez-Herrera, R., 2016. Dehydrated apple matrix supplemented with agave fructans, inulin, and oligofructose. Food Sci. Technol. 65, 1059–1065. https://doi.org/10.1016/j.lwt.2015.09.037.

Hawker, J.S., Hatch, M.D., 1966. A specific sucrose phosphatase from plant tissues. Biochem. J. 99 (1), 102–107. https://doi.org/10.1042/bj0990102.

Huazano-García, A., López, M.G., 2018. Enzymatic hydrolysis of agavins to generate branched fructooligosaccharides (a-FOS). Appl. Biochem. Biotechnol. 184, 25–34. https://doi.org/10.1007/s12010-017-2526-0.

Ivanović, S., Simić, K., Tešević, V., Vujisić, L., Ljekočević, M., Gođevac, D., 2021. GC-FID-MS based metabolomics to access plum brandy quality. Molecules 26, 1391. https://doi.org/10.3390/molecules26051391.

Jaime, L., Martín-Cabrejas, M.A., Mollá, F.J., López-Andréu, E., Esteban, R.M., 2001. Effect of storage on fructan and fructooligosaccharide of onion (*Allium cepa* L.). J. Agric. Food Chem. 49, 982–988. https://doi.org/10.1021/jf000921t.

Kawakami, A., Yoshida, M., 2002. Molecular characterization of sucrose:sucrose 1-fructosyltransferase and sucrose:fructan 6-fructosyltransferase associated with fructan accumulation in winter wheat during cold hardening. Biosci. Biotechnol. Biochem. 66, 2297–2305. https://doi.org/10.1271/bbb.66.2297.

Kocourek, J., Tichá, M., Koštíř, J., 1966. The use of diphenylamine-aniline-phosphoric acid reagent in the detection and differentiation of monosaccharides and their derivatives on paper chromatograms. J. Chromatogr. A 24, 117–124. https://doi.org/10.1016/S0021-9673(01)98109-9.

Komsta, Ł., 2012. Chemometrics in fingerprinting by means of thin layer chromatography, 2012 Chromatogr. Res. Int., 893246. https://doi.org/10.1155/2012/893246.

Kowkabany, G.N., 1954. Paper chromatography of carbohydrates and related compounds. In: Wolfrom, M.L. (Ed.), Advances in Carbohydrate Chemistry. Academic Press, New York, pp. 303–353.

Li, S.P., Wu, D.T., Lv, G.P., Zhao, J., 2013. Carbohydrates analysis in herbal glycomics. Trends Anal. Chem. 52, 155–169. https://doi.org/10.1016/j.trac.2013.05.020.

Madia, V.N., De Vita, D., Messore, A., Toniolo, C., Tudino, V., De Leo, A., , et al.Costi, R., 2021. Analytical characterization of an inulin-type fructooligosaccharide from root-tubers of *Asphodelus ramosus* L. Pharmaceuticals 14, 278. https://doi.org/10.3390/ph14030278.

Mancilla-Margalli, N.A., López, M.G., 2006. Water-soluble carbohydrates and fructan structure patterns from *Agave* and *Dasylirion* species. J. Agric. Food Chem. 54, 7832–7839. https://doi.org/10.1021/jf060354v.

Márquez-López, R.E., Santiago-García, P.A., López, M.G., 2022. Agave fructans in Oaxaca's emblematic specimens: *Agave angustifolia* Haw. and *Agave potatorum* Zucc. Plants 11, 1834. https://doi.org/10.3390/plants11141834.

Martínez-Gamiño, D., García-Soto, M.J., González-Acevedo, O., Godínez-Hernández, C., Juárez-Flores, B., Ortiz-Basurto, R.I., Rodríguez-Aguilar, Maribel, Flores-Ramírez, R., Martínez-Martínez, M., Ratering, S., Schnell, S., Bach, H., Martínez-Gutiérrez, F., 2022. Prebiotic effect of fructans from *Agave salmiana* on probiotic lactic acid bacteria and in children as a supplement for malnutrition. Food Funct. 13, 4184–4193. https://doi.org/10.1039/D1FO03852D.

Matros, A., Peukert, M.J., Lahnstein, U., Seiffert, R., Burton, 2019. Determination of fructans in plants: current analytical means for extraction, detection, and quantification. Annu. Plant Rev. 2, 1–39. https://doi.org/10.1002/9781119312994.apr0672.

Mellado-Mojica, E., López, M.G., 2012. Fructan metabolism in *A. tequilana* Weber blue variety along its developmental cycle in the field. J. Agric. Food Chem. 60, 11704–11713. https://doi.org/10.1021/jf303332n.

Milojković-Opsenica, D., Ristivojević, P., Trifković, J., Vovk, I., Lušić, D., Tešić, Ž., 2016. TLC fingerprinting and pattern recognition methods in the assessment of authenticity of poplar-type propolis. J. Chromatogr. Sci. 54, 1077–1083. https://doi.org/10.1093/chromsci/bmw024.

Morlock, G.E., Sabir, G., 2011. Comparison of two orthogonal liquid chromatographic methods for quantitation of sugars in food. J. Liq. Chromatogr. Relat. 34, 902–919. https://doi.org/10.1080/10826076.2011.571118.

Morlock, G.E., Ristivojević, P., Chernetsova, E.S., 2014. Combined multivariate data analysis of high-performance thin-layer chromatography fingerprints and direct analysis in real time mass spectra for profiling of natural products like propolis. J. Chromatogr. A 1328, 104–112. https://doi.org/10.1016/j.chroma.2013.12.053.

Nobre, C., Teixeira, J.A., Rodrigues, L.R., 2013. New trends and technological challenges in the industrial production and purification of fructo-oligosaccharides. Crit. Rev. Food Sci. Nutr. 55, 1444–1455. https://doi.org/10.1080/10408398.2012.697082.

Oomen, W.W., Begines, P., Mustafa, N.R., Wilson, E.G., Verpoorte, R., Choi, Y.H., 2020. Natural deep eutectic solvent extraction of flavonoids of *Scutellaria baicalensis* as a replacement for conventional organic solvents. Molecules 25, 617. https://doi.org/10.3390/molecules25030617.

Pérez-López, A.V., Simpson, J., Clench, M.R., Gomez-Vargas, A.D., Ordaz-Ortiz, J.J., 2021. Localization and composition of fructans in stem and rhizome of *Agave tequilana* Weber var. azul. Front. Plant Sci. 11, 608850 https://doi.org/10.3389/fpls.2020.608850.

Qiu, F., Imai, A., McAlpine, J.B., Lankin, D.C., Burton, I., Karakach, T., Farnsworth, N.R., Chen, S.N., Pauli, G.F., 2012. Dereplication, residual complexity, and rational naming: the case of the Actaea triterpenes. J. Nat. Prod. 75, 432–443. https://doi.org/10.1021/np200878s.

Reiffová, K., Nemcová, R., 2006. Thin-layer chromatography analysis of fructooligosaccharides in biological samples. J. Chromatogr. A 1110, 214–221. https://doi.org/10.1016/j.chroma.2006.01.039.

Ristivojević, P., Andrić, F.L., Trifković, J., Vovk, I., Stanisavljević, L.Ž., Tešić, Ž.L., Milojković-Opsenica, D.M., 2014. Pattern recognition methods and multivariate image analysis in HPTLC fingerprinting of propolis extracts. J. Chemom. 28, 301–310. https://doi.org/10.1002/cem.2592.

Ritsema, T., Joling, J., Smeekens, S., 2003. Patterns of fructan synthesized by onion fructan:fructan 6G-fructosyltransferase expressed in tobacco BY2 cells - is fructan : fructan 1-fructosyltransferase needed in onion? New Phytol. 160, 61–67. https://doi.org/10.1046/j.1469-8137.2003.00858.x.

Ruíz-Matute, A.I., Hernández-Hernández, O., Rodríguez-Sánchez, S., Sanz, M.L., Martínez-Castro, I., 2011. Derivatization of carbohydrates for GC and GC-MS analyses. J. Chromatogr. B 879, 1226–1240. https://doi.org/10.1016/j.jchromb.2010.11.013.

Salinas, C., Handford, M., Pauly, M., Dupree, P., Cardemil, L., 2016. Structural modifications of fructans in *Aloe barbadensis* Miller (*Aloe vera*) grown under water stress. PLoS One 11, e0159819. https://doi.org/10.1371/journal.pone.0159819.

Salomé-Abarca, L.F., van der Pas, J., Kim, H.K., van Uffelen, G.A., Klinkhamer, P.G.L., Choi, Y.H., 2018. Metabolic discrimination of pine resins using multiple analytical platforms. Phytochemistry 155, 37–44. https://doi.org/10.1016/j.phytochem.2018.07.011.

Salomé-Abarca, L.F., Mandrone, M., Sanna, C., Poli, F., van der Hondel, C.A., Klinkhamer, P.G.L., Choi, Y.H., 2020. Metabolic variation in *Cistus monspeliensis* L. ecotypes correlated to their plant-fungal interactions. Phytochemistry 176, 112402. https://doi.org/10.1016/j.phytochem.2020.112402.

Salomé-Abarca, L.F., Gođevac, D., Kim, M.S., Hwang, G.S., Park, S.C., Jang, Y.P., Van Den Hondel, C.A.M.J.J., Verpoorte, R., Klinkhamer, P.G.L., Choi, Y.H., 2021. Latex metabolome of Euphorbia species: geographical and inter-species variation and its proposed role in plant defense against herbivores and pathogens. J. Chem. Ecol. 47 (6), 564–576.

Santiago-García, P.A., Mellado-Mojica, E., León-Martínez, F.M., Dzul-Cauich, J.G., López, M.G., García-Vieyra, M.I., 2021. Fructans (agavins) from *Agave angustifolia* and *Agave potatorum* as fat replacement in yogurt: effects on physicochemical, rheological, and sensory properties. Food Sci. Technol. 140, 110846 https://doi.org/10.1016/j.lwt.2020.110846.

Schwimmer, S., Bevenue, A., 1956. Reagent for differentiation of 1,4-and 1,6-linked glucosaccharides. Science 123, 543–544, 0.1126/science.123.3196.543.

Shawky, E., Abou, R.M., Kheir, E., 2018. Rapid discrimination of different Apiaceae species based on HPTLC fingerprints and targeted flavonoids determination using multivariate image analysis. Phytochem. Anal. 29, 452–462. https://doi.org/10.1002/pca.2749.

Shetty, N., Gislum, R., Jensen, A.M.D., Boelt, B., 2012. Development of NIR calibration models to assess year-to-year variation in total non-structural carbohydrates in grasses using PLSR. Chemometr. Intell. Lab. Syst. 111, 34–38. https://doi.org/10.1016/j.chemolab.2011.11.004.

Shiomi, N., Onodera, S., Chatterton, N.J., Harrison, P.A., 1991. Separation of fructooligosaccharide isomers by anion-exchange chromatography. Agric. Biol. Chem. 55, 1427–1428. https://doi.org/10.1271/bbb1961.55.1427.

Simion, I.M., Casoni, D., Sârbu, C., 2019. Classification of Romanian medicinal plant extracts according to the therapeutic effects using thin layer chromatography and robust chemometrics. J. Pharm. Biomed. Anal. 163, 137–143. https://doi.org/10.1016/j.jpba.2018.09.047.

Versluys, M., Kirtel, O., Toksoy-Öner, E., Van den Ende, W., 2018. The fructan syndrome: evolutionary aspects and common themes among plants and microbes. Plant Cell Environ. 41, 16–38. https://doi.org/10.1111/pce.13070.

Yildiz, S., 2010. The metabolism of fructooligosaccharides and fructooligosaccharide-related compounds in plants. Food Rev. Int. 27, 16–50. https://doi.org/10.1080/87559129.2010.518295.

Zhao, J., Deng, Y., Li, S.P., 2017. Advanced analysis of polysaccharides, novel functional components in food and medicine dual purposes Chinese herbs. Trends Anal. Chem. 96, 138–150. https://doi.org/10.1016/j.trac.2017.06.006.